EPJ Web of Conferences **274**, 05006 (2022) https://doi.org/10.1051/epjconf/202227405006
XVth Quark Confinement and the Hadron Spectrum

Charm quark fugacity in hot QCD

Valeriya Mykhaylova[1,*]

[1]Institute of Theoretical Physics, University of Wrocław, PL-50204 Wrocław, Poland

Abstract. We study the fugacity of charm quarks in hot QCD from the quasiparticle perspective. The system is described in terms of dynamical quarks and gluons dressed by the effective temperature-dependent masses which link the thermodynamics of the model to the lattice QCD data for $N_f = 2 + 1$. We insert the charm quarks „by hand" and investigate how their scatterings with the quasiparticles affect the charm quark fugacity in a viscous medium expanding in all spatial dimensions and in the perfect fluid propagating longitudinally. We find that the charm quark fugacity strongly depends on the evolution of the deconfined matter at early stages while behaving universally close to the QCD crossover.

1 Introduction

The experimental and theoretical studies show that, as predicted in [1], the charm quarks and their bound state, charmonium, can be used as direct probes of the quark-gluon plasma [2, 3]. Therefore it is of high importance to analyze not only the production of charmonium in heavy ion collisions but also the production mechanism of charm quarks in the quark-gluon plasma (QGP). If one describes the QGP in terms of massless quarks and gluons, the charm quark production will be insignificant due to the large amount of energy required to produce the massive charm-anticharm pair [4]. However, if the deconfined medium is expressed in terms of massive (quasi)particles, especially with dynamically generated effective masses, the scatterings among them may significantly increase the charm quark production.

The number of charm quarks can be quantified by the fugacity parameter λ_c which indicates the deviation of the statistical phase space density [5], i.e. it shows how far the charm quarks appear from chemical equilibrium. The goal of this study is to investigate the charm quark fugacity in the expanding hot QCD medium. The system is described in the kinetic quasiparticle framework discussed in Sec. 2, with the time evolution given in Sec. 3. We evaluate the charm quark fugacity by utilizing the rate equation introduced in Sec. 4. The discussion of the numerical results is presented in Sec. 5, with a brief summary in Sec. 6.

2 Quasiparticle Model

We assume the QGP is in thermal and chemical equilibrium and consists of quasiparticles with light (l) (as a sum of degenerate up and down flavors) and strange (s) quarks, as well as gluons (g), i.e. $N_f = 2 + 1$, contributing to the equation of state (EoS) [6]. Alongside,

*e-mail: valeriya.mykhaylova@uwr.edu.pl

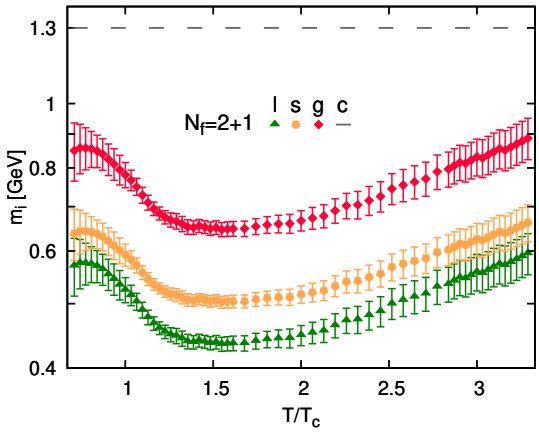

Figure 1. Masses of the QGP constituents as functions of the temperature scaled by the pseudocritical $T_c = 0.155$ GeV.

we introduce the charm quarks into the deconfined medium as „obstacles" which do not contribute to the EoS and have a constant mass $m_c = 1.3$ GeV.

One of the main tools of kinetic theory is the momentum-distribution function f_i. For this study we employ the Jüttner statistics at vanishing chemical potential, $\mu = 0$ [7, 8],

$$f_i(\lambda_i) = \lambda_i \left(e^{E_i/T} \pm \lambda_i \right)^{-1}, \tag{1}$$

where λ_i and E_i is the particle fugacity and energy, respectively, and T is the temperature of the system. Since the quasiparticles are assumed to be chemically equilibrated, they are described by Fermi-Dirac or Bose-Einstein statistics, i.e. $\lambda_{l,s,g} = 1$ in the above equation. The charm quarks are out of chemical equilibrium and the determination of λ_c is one of the main steps of this research. The computation of the charm quark fugacity is discussed in Sec. 4.

The quasiparticle model (QPM) assumes that as a particle propagates through the system and exhibits various in-medium interactions, it becomes dressed by the dynamically generated self-energy Pi_i. Thus, the effective mass of the quasiparticle reads

$$m_i(T) = \left[(m_i^0)^2 + \Pi_i(T) \right]^{1/2}, \tag{2}$$

with the the bare particle mass[1] m_i^0 and the self-energy Π_i depending on the temperature and coupling as [9, 10]

$$\Pi_{l,s}(T) = 2 \left(m_{l,s}^0 \sqrt{\frac{G(T)^2}{6} T^2} + \frac{G(T)^2}{6} T^2 \right), \tag{3}$$

$$\Pi_g(T) = \left(3 + \frac{3}{2} \right) \frac{G(T)^2}{6} T^2, \tag{4}$$

for quarks and gluons, respectively.

Note that the effective temperature-dependent mass, as well as constant charm quark mass, enters the distribution function given by Eq. (1) through the dispersion relation for each (quasi)particle species, $E_i^2 = \vec{p}^{\,2} + m_i^2$.

[1] We use $m_l^0 = 5$ MeV, $m_s^0 = 95$ MeV and $m_g^0 = 0$ for light, strange quarks and gluons, respectively.

We deduce the effective running coupling $G(T)$ from the entropy density computed by lattice gauge theory simulations for $N_f = 2 + 1$ [6, 11]. Our previous studies show that $G(T)$ effectively incorporates the non-perturbative QCD dynamics in the vicinity of the crossover and reproduces the perturbative behavior in the very high-temperature regime [6, 12].

Fig. 1 shows numerical results for the masses of dynamical quarks and gluons, as well as the constant charm quark mass. One can observe that the effective masses of the quasiparticles are much larger than their bare masses. Therefore we expect the scatterings between such massive quasiparticles to generate a significant number of charm quark pairs. For the detailed discussion on m_i we refer the reader to [6].

3 Time evolution

We study the evolution of charm quarks in hot QCD in two different scenarios of the QGP expansion:

i) Longitudinal (1D) propagation of perfect fluid, i.e. Bjorken flow, with time evolution specified by the scaling solution [13]

$$T(\tau) = T_0(\tau_0) \left(\frac{\tau_0}{\tau}\right)^{1/3}, \tag{5}$$

where τ denotes the time, and $T_0(\tau_0)$ is the initial value at which the fireball is created and the hydrodynamics becomes applicable. The pseudocritical temperature is reached at $\tau \simeq 13$ fm.

ii) Longitudinal and transverse, i.e. (2+1)D, expansion of viscous fluid with the time evolution defined by the second order viscous hydrodynamics [14]. The QCD crossover temperature is achieved at $\tau \simeq 11$ fm. The computation incorporates the temperature-dependent specific shear viscosity η/s computed in the QPM under the relaxation time approximation based on the total cross sections between the quasiparticles [6]. The result appears to be in line with η/s obtained from hydrodynamic simulations [14].

Both systems are assumed to be boost-invariant with the initial conditions specified as $T_0 = 0.624$ GeV, $\tau_0 = 0.2$ fm [14].

4 Rate equation

To find how the fugacity of charm quarks (λ_c) changes with temperature and time, we utilize the rate equation of the following form [8, 15]:

$$\partial_\mu [n_c(\lambda_c)\, u^\mu] = R_c \left[1 - \left(\frac{n_c(\lambda_c)}{n_c^0}\right)^2\right], \tag{6}$$

$$n_i(\lambda_i) = d_i \int \frac{d^3p}{(2\pi)^3} f_i(\lambda_i), \tag{7}$$

$$R_c = \frac{1}{2}\, \bar{\sigma}_{gg\to c\bar{c}}\, n_g^2 + \bar{\sigma}_{l\bar{l}\to c\bar{c}}\, n_l^2 + \bar{\sigma}_{s\bar{s}\to c\bar{c}}\, n_s^2. \tag{8}$$

Here, n_i is the number density computed by integrating the distribution function over the phase-space, with the spin-color degeneracy factor d_i; $n_c^0 = n_c(\lambda_c = 1)$ is the charm quark number density in equilibrium. R_c is the production rate of charm quarks based on thermal-averaged cross sections, $\bar{\sigma}_{ii'\to jj'}$, computed at the leading order for massive (quasi)particles. In contrast to our previous studies [6, 12], where we have computed transport (large-angle scattering) cross sections [16], this research incorporates the total cross sections. The factor of $1/2$ in Eq. (8) is needed to avoid the double counting of gluons [5]. Additionally, Eq. (6)

satisfies the assumption that as charm quarks reach the chemical equilibrium, the charm production and annihilation rates become equal [15].

Assuming a purely longitudinal propagation, one can rewrite the left-hand side (LHS) of Eq. (6) for *i*) scenario as [5, 8],

$$\partial_\mu[n_c(\lambda_c)\,u^\mu] = u^\mu\partial_\mu n_c + n_c\partial_\mu u^\mu = \frac{\partial n_c}{\partial\tau} + \frac{n_c}{\tau}. \tag{9}$$

For (2+1)D evolution in *ii*), the flow velocity changes because of the additional propagation in the transverse plane. Following [15, 17], we express the flow velocity in cylindrical coordinates and rewrite the LHS of Eq. (6) as

$$\partial_\mu[n_c(\lambda_c)\,u^\mu] = \frac{1}{\tau\,R^2(\tau)}\frac{\partial}{\partial\tau}\left(\tau\,R^2(\tau)\,n_c(\lambda_c)\,\langle u^\tau\rangle\right), \tag{10}$$

where $R(\tau)$ is the transverse radius of the system given by

$$R(\tau) = R_0 + a(\tau-\tau_0)^2. \tag{11}$$

We apply $R_0(\tau_0) = 7$ fm for the initial radius and $a = 0.043$ fm^{-1} for the transverse acceleration. This value satisfies the condition of the QGP evolution in (2+1)D, where it hadronizes at $\tau \simeq 11$ fm [18]. Further, $\langle u^\tau\rangle$ is the averaged time component of the four-velocity, which can be expressed in terms of the transverse radius as [17, 19]

$$\langle u^\tau\rangle = \frac{2}{R^2(\tau)}\int_0^{R(\tau)} dr\left[\left(\frac{dR(\tau)}{d\tau}\right)^2\frac{r}{R(\tau)}\right]^{-1/2}. \tag{12}$$

Once the LHS of Eq. (6) is rewritten as shown in Eq. (9) or Eq. (10), we solve it numerically for different initial values of charm quark fugacity λ_c. The results are shown in Fig. 2 and Fig. 3.

5 Charm quark fugacity

The time evolution of the charm quark fugacity is presented in Fig. 2. In perfect QGP undergoing the Bjorken flow (the *i*) case), the charm quark fugacity first exhibits an increase with time, and then starts to decrease, independently of the initial value λ_0. The turning point becomes less sharp and shifts towards higher τ for lower λ_0. In contrast to that, in the *ii*) scenario for (2+1)D expansion of viscous QGP, all the $\lambda_c(\tau)$ are flattened and as τ grows, the solutions either slowly increase (for $\lambda_0 \ll 1$) or smoothly decrease (for $\lambda_0 \gtrapprox 10$) on the whole examined range. For the intermediate values of λ_0, one can observe a behavior similar to $\lambda_c(\tau)$ in the *i*) scenario but with a less pronounced turning point.

We additionally observe that for *i*) and *ii*) evolutions individually, all the $\lambda_c(\tau)$ tend to overlap each other at high τ. Such a tendency may be related to the universal behavior of the solutions of the differential equations when there exists a particular attractor to which all the solutions converge [20].

Fig. 3 exhibits numerical results for the charm quark fugacity as a function of temperature. The T axis is reversed to correspond to the horizontal (time) axis in Fig. 2. As a function of temperature, we see that all the fugacities first increase with the decreasing T and then start to drop until they reach the common universal solution for *i*) and *ii*) evolutions separately. At the pseudocritical temperature, $\lambda_c \neq 1$, therefore in the QPM, the charm quarks will not reach the chemical equilibrium. In addition, at $T \simeq 0.2$ GeV and below, the hierarchy

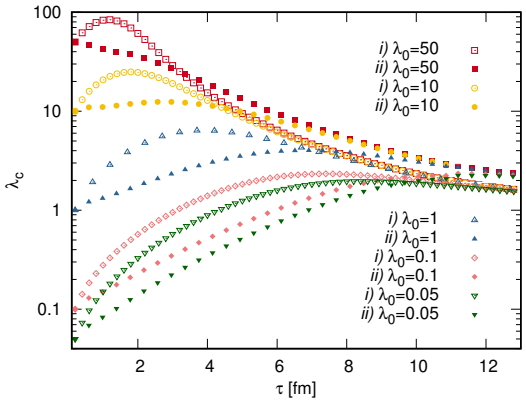

Figure 2. Charm quark fugacity as a function of time for different initial values λ_0. The open bullets show λ_c in the *i*) case of perfect QGP propagating longitudinally, while full symbols represent the *ii*) evolution of hot QCD medium expanding in (2+1)D, with temperature-dependent shear viscosity taken into account.

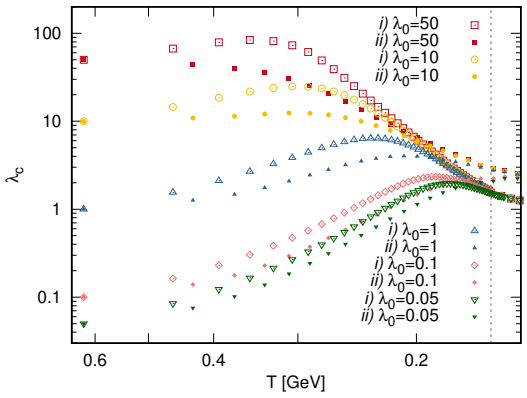

Figure 3. Charm quark fugacity λ_c as a function of temperature for different initial values λ_0. The symbols and colors correspond to that in Fig. 2. The dashed line represents the pseudocritical temperature.

between the $\lambda_c(T)$ curves in *i*) and *ii*) case changes, and the fugacity in (2+1)D viscous QGP becomes larger than in 1D perfect medium, independently of the initial λ_0. This leads us to the conclusion that at the final stage of the QGP evolution, the number of charm quarks is higher when the QGP expands in all spatial dimensions with the shear viscosity taken into account.

6 Conclusions

We have explored the evolution of the charm quark fugacity λ_c in hot QCD medium with $N_f = 2 + 1$ quark flavors. The calculations are performed in the well-grounded quasiparticle model (QPM) which describes the deconfined matter in terms of the dynamical quarks and gluons with effective masses linked to the lattice QCD thermodynamics. For the evolution of the QGP, we have adopted the result of hydrodynamic simulations of the viscous QGP expanding in all spatial dimensions, i.e. (2+1)D. We additionally juxtapose this result to the longitudinal propagation (1D) of the perfect fluid.

We have solved the rate equation for the charm quark fugacity λ_c and observed that its behavior depends significantly on the QGP evolution scenario at early stages, while as the system approaches the crossover, the dynamics of λ_c becomes universal. Independently of the initial fugacity λ_0, in the QPM all the solutions of the rate equation are attracted to the same value, individual for 1D and (2+1)D expansions. At the QCD pseudocritical temperature, the charm quark fugacities do not reach unity which indicates that the charm quarks do not achieve the chemical equilibrium before the hadronic phase. The results of this research may be used to study the charm quark production in the deconfined medium, as well as to investigate the hydrodynamic attractor for the solutions of the rate equation [18].

7 Acknowledgements

This work was done in collaboration with Chihiro Sasaki and Krzysztof Redlich, whom I would like to thank for a generous support and the scientific guidance. This work was partly supported by the Polish National Science Center under the OPUS 16 Grant No. 2018/31/B/ST2/01663 and under the PRELUDIUM 20 Grant No. UMO-2021/41/N/ST2/02615.

References

[1] T. Matsui, H. Satz, Phys. Lett. B **178**, 416 (1986)
[2] A. Andronic, P. Braun-Munzinger, K. Redlich, J. Stachel, Nature **561**, 321 (2018), 1710.09425
[3] R. Rapp, D. Blaschke, P. Crochet, Prog. Part. Nucl. Phys. **65**, 209 (2010), 0807.2470
[4] P. Levai, R. Vogt, Phys. Rev. C **56**, 2707 (1997), hep-ph/9704360
[5] P. Koch, B. Muller, J. Rafelski, Phys. Rept. **142**, 167 (1986)
[6] V. Mykhaylova, M. Bluhm, K. Redlich, C. Sasaki, Phys. Rev. D **100**, 034002 (2019), 1906.01697
[7] F. Jüttner, Annalen der Physik **339**, 856 (2006)
[8] T.S. Biro, E. van Doorn, B. Muller, M.H. Thoma, X.N. Wang, Phys. Rev. C **48**, 1275 (1993), nucl-th/9303004
[9] M. Bluhm, B. Kampfer, R. Schulze, D. Seipt, Eur. Phys. J. C **49**, 205 (2007), hep-ph/0608053
[10] R.D. Pisarski, Nucl. Phys. A **498**, 423C (1989)
[11] S. Borsanyi, Z. Fodor, C. Hoelbling, S.D. Katz, S. Krieg, K.K. Szabo, Phys. Lett. B **730**, 99 (2014), 1309.5258
[12] V. Mykhaylova, C. Sasaki, Phys. Rev. D **103**, 014007 (2021), 2007.06846
[13] J.D. Bjorken, Phys. Rev. D **27**, 140 (1983)
[14] J. Auvinen, K.J. Eskola, P. Huovinen, H. Niemi, R. Paatelainen, P. Petreczky, Phys. Rev. C **102**, 044911 (2020), 2006.12499

[15] B.W. Zhang, C.M. Ko, W. Liu, Phys. Rev. C **77**, 024901 (2008), 0709.1684
[16] P. Danielewicz, M. Gyulassy, Phys. Rev. D **31**, 53 (1985)
[17] L. Alvarez-Ruso, V. Koch, Phys. Rev. C **65**, 054901 (2002), nucl-th/0201011
[18] C.S. V.Mykhaylova, K. Redlich, *To appear on ArXiv* (2022)
[19] E. Schnedermann, J. Sollfrank, U.W. Heinz, Phys. Rev. C **48**, 2462 (1993), nucl-th/9307020
[20] M.P. Heller, M. Spalinski, Phys. Rev. Lett. **115**, 072501 (2015), 1503.07514